Analysis and Application of Fourier-Gegenbauer Method to Stiff Differential Equations *

appeared in SIAM J. Numerical Analysis, 33:5 (1996), 1844-1863

A. Averbuch†, M. Israeli‡, L. Vozovoi‡

† School of Mathematical Sciences, Tel Aviv University, Tel Aviv 69978, Israel

‡ Faculty of Computer Science, Technion, Haifa 32000, Israel

Abstract

The Fourier-Gegenbauer (FG) method, introduced by [1], is aimed to remove the Gibbs phenomenon, that is to recover the point values of a non-periodic function from its Fourier coefficients. In this paper we discuss some numerical aspects of the FG method related to its *pseudospectral* implementation. In particular, we analyze the convergence of finite Gegenbauer series with hundreds terms, suitable for computations. We also demonstrate the capability of the FG method for getting a spectrally accurate approximation on small sub-intervals for functions who are rapidly oscillating or have steep profiles.

Bearing on the previous analysis, we suggest a high-order spectral Fourier method for the solution of non-periodic differential equations. It includes a polynomial subtraction technique to accelerate the convergence of the Fourier series and the FG algorithm to evaluate derivatives on the boundaries of non-periodic functions. The current Hybrid Fourier-Gegenbauer method possesses better resolution properties than the original FG method. The precision of this method is demonstrated by solving stiff elliptic problems with steep solutions.

1 Introduction

Spectral methods are widely used in computational fluid dynamics due to their fast (exponential) convergence with the number of degrees of freedom. These methods use series expansions in terms of orthogonal polynomials or trigonometric functions. The spectral Fourier method is best suitable for the evaluation of spatial derivatives, because the differential operators are represented in the transform space by diagonal matrices and thus they do not couple harmonics with different wave numbers. This method also allows the fast Fourier transforms (FFT) to move between physical and Fourier spaces.

The exponential convergence takes place, however, only if the Fourier transform operates on periodic C^∞- functions. For non-periodic problems, for example, viscous problems with no-slip boundary conditions, periodically extended functions will have discontinuity on the

*This research of the first author was supported partly by a grant from Tel Aviv University for 1995-1996

boundaries. In such a case Fourier series converges very slowly with the number of modes N (like $O(N^{-1})$) inside the interval, and does not converge near the boundaries, where the spurious oscillations of the order $O(1)$ will occur- Gibbs phenomenon.

Nevertheless, the Fourier method can be employed for the solution of non-periodic problems along with appropriate smoothing procedure. In [8, 12] the smoothing is attained by subtraction of polynomials such that a residual function and several of its derivatives vanish on the boundaries. In order to construct a subtraction polynomial the derivatives of the original function on the boundaries must be known explicitly. Although a "smoothed" function is not analytic and thus its corresponding Fourier series converges algebraically, in practice the rate of convergence may be quite satisfactory even with a small order subtraction polynomial.

In [1, 2] it was shown that the first $2N+1$ Fourier coefficients of analytic but non-periodic function contain enough information to construct a spectrally accurate interpolant. The basic concept of this approach is to re-expand slowly convergent Fourier partial sums into rapidly convergent Gegenbauer series. The exponential convergence of such polynomial series has been proven for the limit of large number of terms. In [4] this algorithm was implemented for the solution of boundary value problems with smooth non-periodic source function.

The resolution properties of the Fourier-Gegenbauer (FG) method are found to be worse than those of the Fourier or Chebyshev spectral methods [2]: a minimum 22.2 points per wavelength is needed to assure exponential convergence (in comparison with 2 points in the Fourier and π points in the Chebyshev methods). Therefore, the FG approximation of highly oscillating components in the function requires fairly large number of terms in the Gegenbauer expansion. In addition, by using this algorithm, the computation of the high-order terms is subject to round-off effects. As a result, the FG method is incapable to resolve large gradients in the solution.

In the current paper we analyze some of the numerical aspects of the FG method, related to *pseudospectral* (collocation) version of this method. In this case, we are given the first $2N+1$ Fourier coefficients of the interpolant, whereas in the Galerkin method the information is given by the $2N+1$ Fourier coefficients of the function itself. Here, we focus on the analysis of finite Gegenbauer series, truncated after m terms, where $m \sim 100$ (computations with larger m are beyond the capacity of modern computers). In the representative case of the wave function $f(x) = e^{i\pi\omega x}$, we found that the convergence of this series is not monotonic. Furthermore, the amplitude of the largest term in the Gegenbauer expansion grows exponentially with ω.

When dealing with a collocation method, the presence of high frequency components in the function is unavoidable due to round-off errors. Such a computational "noise" has the maximum spatial frequency $\omega \sim N$. Though, the amplitude of the "noise" is very small, (of order $\sim 10^{-16}$ for computations with double precision), the rapid amplification of the Gegenbauer terms along the series causes a loss of accuracy at moderately large $m \approx \pi\omega$, where $\omega \approx N$ (however, the convergence takes place asymptotically for $m \to \infty$).

We propose a modification of the FG algorithm which allows us to treat accurately non-periodic problems with steep or rapidly oscillating solutions. The new algorithm incorporates several techniques. The FG method is implemented and evaluated only on the two extreme sub-intervals, within spectral accuracy, several of the lowest derivatives on the boundaries. Within the range of each of these intervals, the functions are *smooth* enough to assure *fast* convergence of the FG algorithm (the last property is necessary for keeping a relatively *small* number of terms in the Gegenbauer expansion to prevent the amplification of "noise"). Then, the ordinary Fourier spectral method is carried out on the whole interval along with a polynomial subtraction procedure in order to accelerate the convergence of the Fourier series. The current Fourier method has substantial benefit to our spectral multidomain approaches [5, 6, 7], which make use of the Local Fourier Basis technique.

The paper has the following structure: The basic Fourier-Gegenbauer algorithm is described in section 2. The results on convergence and resolution properties of the FG method in the limit of large N and m are summarized in section 3. In section 4 we discuss some aspects of the pseudospectral formulation of the FG method. The convergence of finite Gegenbauer series for the wave function is analyzed in section 5. The ability of the FG method to evaluate accurately the local quantities is discussed in section 6. Finally, a modified (hybrid) Fourier-Gegenbauer method for the solution of non-periodic differential equations is presented in section 7.

2 Fourier-Gegenbauer Method

In this section we outline the basics foundations of the Fourier-Gegenbauer method that was developed by D. Gottlieb et. al. in [1, 2, 3], which constitutes an essential component for the current algorithm.

Consider a non-periodic analytic function $f(x)$ defined on $[-1,1]$. Such a function has discontinuities at the boundaries $x = \pm 1$ if it is extended periodically with period 2. The Fourier coefficients of $f(x)$ are given by

$$\hat{f}(k) = \frac{1}{2}\int_{-1}^{1} f(x)e^{-ik\pi x}dx. \tag{2.1}$$

Assume that the first $2N+1$ Fourier coefficients $\hat{f}(k)$ are given. Our objective is to recover the function $f(x)$ on $x \in [-1,1]$ with exponential accuracy in the maximum norm.

The truncated Fourier series for a discontinuous function $f(x)$

$$f_N(x) = \sum_{k=-N}^{N} \hat{f}(k)e^{ik\pi x}, \tag{2.2}$$

converges slowly, like $O(\frac{1}{N})$, inside the interval and exhibits $O(1)$ spurious oscillations near the boundaries $x = \pm 1$ (known as Gibbs phenomenon). Thus, there is no convergence in the maximum norm.

The basic approach of [1] is based on the re-expansion of (2.2) into rapidly convergent Gegenbauer series

$$f(x) = \sum_{l=0}^{\infty} \hat{f}^{\lambda}(l)C_l^{\lambda}(x) \tag{2.3}$$

where $C_l^\lambda(x)$ is a two-parametric family of the Gegenbauer polynomials (l is the order of the polynomial, λ is a parameter; the numerical algorithm for the computation of the polynomials $C_l^\lambda(x)$ are given in [9], page 782).

The Gegenbauer coefficients are defined by

$$\hat{f}^\lambda(l) = \frac{1}{h_l^\lambda}\int_{-1}^{1}(1-x^2)^{\lambda-\frac{1}{2}}f(x)C_l^\lambda(x)dx \tag{2.4}$$

where

$$h_l^\lambda = \pi^{\frac{1}{2}}C_l^\lambda(1)\frac{\Gamma(\lambda+1)}{\Gamma(\lambda)(l+\lambda)}.$$

Since we do not know the function $f(x)$, but only its truncated Fourier series (2.2), we have only an approximation to $\hat{f}^\lambda(l)$ which we denote by $\hat{g}_N^\lambda$, given by

$$\hat{g}_N^\lambda(l) = \frac{1}{h_l^\lambda}\int_{-1}^{1}(1-x^2)^{\lambda-\frac{1}{2}}f_N(x)C_l^\lambda(x)dx. \tag{2.5}$$

It is remarkable that the approximated Gegenbauer coefficients $\hat{g}_N^\lambda(l)$ can be explicitly expressed in terms of the Fourier coefficients $\hat{f}(k)$ as follows:

$$\hat{g}_N^\lambda(l) = \delta_{0l}\hat{f}(0) + \Gamma(\lambda)i^l(l+\lambda)\sum_{0<|k|\leq N} J_{l+\lambda}(\pi k)\left(\frac{2}{\pi k}\right)^\lambda \hat{f}(k) \tag{2.6}$$

where $\Gamma(\lambda)$ and $J_n(x)$ are the Gamma and the Bessel functions. The corresponding Gegenbauer expansion, based on the approximated coefficients $g_N^\lambda(l)$, are:

$$f_{m,N}^\lambda(x) = \sum_{l=0}^{m}\hat{g}_N^\lambda(l)C_l^\lambda(x). \tag{2.7}$$

We refer to (2.6) and (2.7) as the *Fourier-Gegenbauer* (FG) approximation of $f(x)$.

The difference between the Gegenbauer partial sum with m terms of the function $f(x)$

$$f_m^\lambda(x) = \sum_{l=0}^{m}\hat{f}^\lambda(l)C_l^\lambda(x) \tag{2.8}$$

and that of the truncated Fourier series $f_N(x)$ is called *truncation error*:

$$\begin{aligned} TE(x,\lambda,m,N) &= | f_m^\lambda(x) - f_{m,N}^\lambda(x) | \\ &= \left|\sum_{l=0}^{m}(\hat{f}^\lambda(l) - \hat{g}_N^\lambda(l))C_l^\lambda(x)\right|. \end{aligned} \tag{2.9}$$

It measures the error for the finite Gegenbauer expansion due to truncation of the Fourier series. Note that for the "wave" function $e^{i\pi\omega x}$, $\omega \in \mathbf{Z}$ the truncation error $TE(x,\lambda,m,N) \equiv 0$ for all $N \geq \omega$ since in this case $\hat{f}_N = \hat{f}$ and, according to Eqs.(2.4), (2.5), $\hat{f}^\lambda(l) = \hat{f}_N^\lambda(l)$.

The total error of the FG approximation is

$$E(x,\lambda,m,N) = | f(x) - f_{m,N}^\lambda(x) | \tag{2.10}$$

and this can be splitted into two components as follows:

$$
\begin{aligned}
| f(x) - f_{m,N}^{\lambda}(x) | &= | f(x) - f_m^{\lambda}(x) + f_m^{\lambda}(x) - f_{m,N}^{\lambda}(x) | \\
&\leq | f(x) - f_m^{\lambda}(x) | + | f_m^{\lambda}(x) - f_{m,N}^{\lambda}(x) | \, . \qquad (2.11)
\end{aligned}
$$

The second component is the truncation error (2.9). The first component

$$RE(x, \lambda, m, N) = \left| \sum_{l=0}^{\infty} \hat{f}^{\lambda}(l) C_l^{\lambda}(x) - \sum_{l=0}^{m} \hat{f}^{\lambda}(l) C_l^{\lambda}(x) \right| \qquad (2.12)$$

arises due to the truncation of the Gegenbauer series. It is called the *regularization error.*

The FG method can be extended in order to evaluate the derivatives (integrals) of the function $f(x)$ when the Fourier coefficients $\hat{f}(k)$ are known. The algorithm is similar to the one described above, but according to $\hat{f}(k)$ in (2.6), one should take $ik\hat{f}(k)$ for the first derivative, $-k^2\hat{f}(k)$ for the second derivative and so on. The analysis of the approximated error in these cases is given in [4].

We will also need the following relations for the Gegenbauer polynomials:

$$
\begin{aligned}
|C_l^{\lambda}(x)| \ &\leq \ |C_l^{\lambda}(1)|, \qquad x \in [-1, 1] \\
C_l^{\lambda}(1) &= \frac{\Gamma(l + 2\lambda)}{l! \Gamma(2\lambda)} \qquad (2.13)
\end{aligned}
$$

(see [10], page 206 and [9], page 777), and the identity

$$\frac{1}{h_l^{\lambda}} \int_{-1}^{1} (1 - x^2)^{\lambda - \frac{1}{2}} e^{in\pi x} C_l^{\lambda}(x) dx = \Gamma(\lambda) i^l (l + \lambda) J_{l+\lambda}(\pi n) \left(\frac{2}{\pi n} \right)^{\lambda} \qquad (2.14)$$

which can be found in [10], page 213.

3 Asymptotic Convergence and Resolution Properties of the FG Method

In this section we describe the basic results on the convergence of the FG method, derived in [1] and [2]. These results are valid for any analytic function $f(x)$, $x \in [-1, 1]$, whose derivatives satisfy the following estimate:

$$\max_{-1 \leq x \leq 1} \left| \frac{d^k f(x)}{dx^k} \right| \leq C(\rho) \frac{k!}{\rho^k} \qquad (3.1)$$

where $\rho \geq 1$ and $C(\rho)$ are constants, independent of k.

– Both truncation and regularization errors, defined in Eqs.(2.9) and 2.12) correspondingly, attain their maximum at the boundaries $x = \pm 1$.

– At the boundary $x = 1$ the truncation error satisfies the estimate

$$TE(1,\lambda,m,N) \le A\frac{(m+\lambda)\Gamma(m+2\lambda)\Gamma(\lambda)}{(m-1)!\Gamma(2\lambda)}\left(\frac{2}{\pi N}\right)^{\lambda-1}. \tag{3.2}$$

– If $\lambda = \gamma m$ and $m = \beta N$ where γ and β are positive constants, then the truncation error decays exponentially with N as follows:

$$TE(1,\lambda,m,N) \le AN^2 q^N, \qquad q = \left(\frac{\beta^\gamma(1+2\gamma)^{1+2\gamma}}{(2\pi e\gamma)^\gamma}\right)^\beta \tag{3.3}$$

The region of convergence, where $q < 1$, is shown in Fig. 1. The convergence takes place for $\beta < 0.64$.

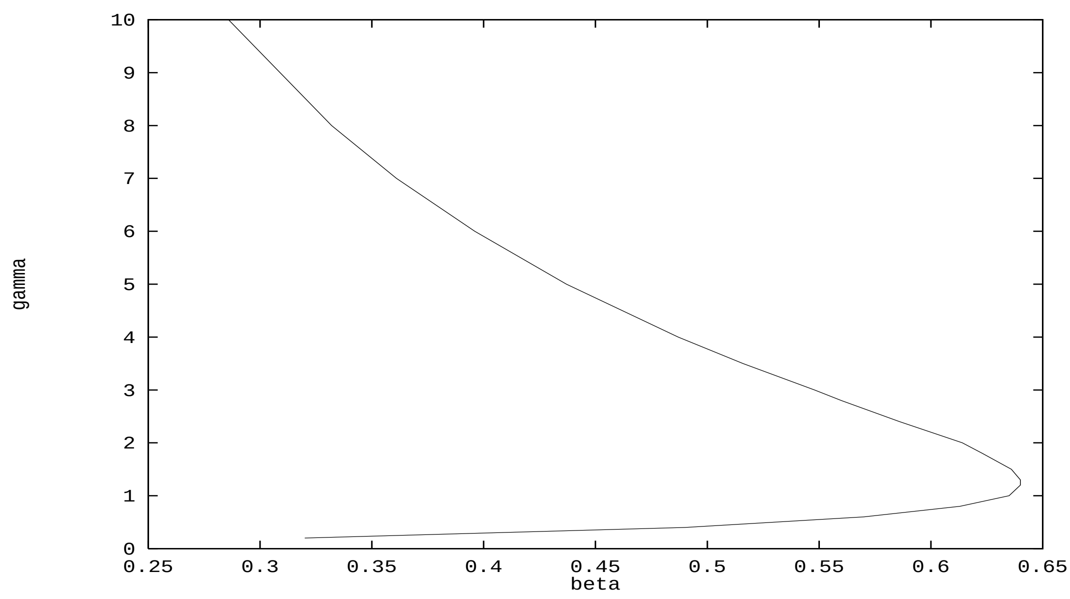

Figure 1: Region of exponential convergence of the Gegenbaur series $q < 1$

– At the boundary $x = 1$, the regularization error satisfies the estimate

$$RE(1,\lambda,m,N) \le A\frac{C(\rho)\Gamma(\lambda)\Gamma(m+2\lambda+1)}{m(2\rho)^{m+1}\Gamma(2\lambda)\Gamma(m+\lambda)} \tag{3.4}$$

For a fixed λ, we can rewrite this expression as follows:

$$RE(1, \lambda, m, N) \leq \tilde{A}(\lambda, \rho)\ m^{\lambda} q^{m}, \qquad q = \frac{1}{2\rho}, \tag{3.5}$$

where $\tilde{A}$ includes all terms, independent of m. The error decays exponentially with m since $q < 1$.

– If $\lambda = \gamma m$, then

$$TE(1, \lambda, m, N) \leq A q^{m}, \qquad q = \frac{(1+2\gamma)^{1+2\gamma}}{\rho 2^{1+2\gamma}\gamma^{\gamma}(1+\gamma)^{1+\gamma}} \tag{3.6}$$

It is easy to verify that q is an increasing function of γ and $q < \frac{1}{\rho} \leq 1$ for all $\gamma > 0$. Thus, the convergence is faster when γ is smaller.

– The resolution properties of the FG method are characterized by the ratio

$$r = \frac{m}{\omega} \tag{3.7}$$

where m is the number of terms required to get an exponentially accurate approximation to the wave function in the Gegenbauer expansion

$$f(x) = e^{i\pi\omega x}, \qquad \omega \in \mathbf{R}^{+} \tag{3.8}$$

(here the wave number $\omega > 0$ is not necessarily an integer).

For constants r and λ, the estimate for the resolution error is similar to that in Eq.(3.5), where $q(\pi/r)$ depends on r. For $r > \pi$, the factor $q < 1$ and thus the exponential convergence takes place.

– If $\gamma = \lambda/m$ is constant, then, the minimum number of Gegenbauer terms per wave, required to resolve the wave function with spectral accuracy, grows with γ. Thus, $r = \pi$ for $\gamma \ll 1$, $r = 7.03$ for $\gamma = 1$, and $r = 8.1$ for $\gamma = 5$. In a slightly different form, the necessary relation between m and ω writes

$$m = \beta(\gamma)\pi\omega, \qquad 1 < \beta(\gamma) < 2.6 \tag{3.9}$$

– In a particular case for the wave function Eq.(3.8) and for r, γ and β are constants, the truncation error decreases exponentially with N if the number of Fourier harmonics per wave, $R = \frac{2N}{\omega}$, is large enough. It is $R_{min} = 22.2$ at $\gamma = 1$ and more for $\gamma < 1$ or $\gamma > 1$.

The above results prove the spectral convergence of the FG approximation for $m \to \infty$, $N \to \infty$. The actual number of terms, needed to reduce the error due to the factor q^{-m} (or q^{-N}), may be considerably large if the coefficients $C(\rho), A, \tilde{A}$ in the previous estimates are large (this is the case of high-frequency wave function, see section 4). In practice, the computation of the Gegenbauer series is limited to $m,\ \lambda \sim 100$ due to the presence of Gamma and Bessel functions in Eqs.(2.6), (2.13). In addition, the computation of high order terms is subject to round-off effects.

Therefore, in this paper we raise the natural question about the behavior of finite Gegenbauer series with moderately large ($m < 100$) number of terms. Also, we are interested in the case when ω is fixed, which is essentially different from the above case $\omega \propto m$. This issue will be discussed in section 5.

4 Pseudospectral Version of the FG method

Another aspect of the FG method considered here is the pseudospectral (collocation) implementation of this method. In this case we deal with truncated Fourier series (Eq.(2.2)), constructed by the collocation procedure rather than by the Galerkin procedure. Thus, the collocation FG approximation is subject to an additional error, caused by the approximated numerical integration in Eq.(2.1). Let $\hat{f}_C(k)$ be the approximated Fourier coefficients, computed by the collocation method. If we are given the grid point values of the function $f(x_j)$ on a $2N+1$ collocation grid, we can compute $\hat{f}_C(k)$ using the Discrete Fast Fourier Transform (DFFT). Of course, in such a case there is no need to reconstruct the interpolant using the FG algorithm, but the Fourier coefficients can be employed to compute the derivatives of $f(x)$ (see section 5).

Using $\hat{f}_C(k)$ we can construct the interpolant $f_{N,C}(x)$, the Gegenbauer coefficients $g^\lambda_{N,C}(l)$ and the FG approximation $f^\lambda_{m,N,C}(x)$ in the collocation case by analogy with Eqs.(2.2), (2.5) and (2.7). The *collocation* error, defined by

$$\begin{aligned} CE(x,\lambda,m,N) &= \mid f^\lambda_{m,N,C}(x) - f^\lambda_{m,N}(x) \mid \\ &= \sum_{l=0}^{m} \left(\hat{g}^\lambda_{N,C}(l) - \hat{g}^\lambda_{N}(l) \right) C^\lambda_l(x) \end{aligned} \tag{4.1}$$

can be estimated as follows:

$$\begin{aligned} \mid CE(x,\lambda,m,N) \mid &\leq \max_{-1\leq x\leq 1} \sum_{l=0}^{m} \left| \hat{g}^\lambda_{N,C}(l) - \hat{g}^\lambda_{N}(l) \right| \left| C^\lambda_l(x) \right| \\ &\leq \sum_{l=0}^{m} \frac{C^\lambda_l(1)}{h_l} \int_{-1}^{1} \left| f_{N,C}(x) - f_N(x) \right| (1-x^2)^{\lambda-\frac{1}{2}} C^\lambda_l(x) dx \\ &= \sum_{l=0}^{m} \frac{C^\lambda_l(1)}{h_l} \sum_{|k|\leq N} \left| \hat{f}_C(k) - \hat{f}(k) \right| \int_{-1}^{1} (1-x^2)^{\lambda-\frac{1}{2}} e^{i\pi k x} C^\lambda_l(x) dx \\ &= \sum_{l=0}^{m} C^\lambda_l(1)\Gamma(\lambda) \sum_{|k|\leq N} \left| \hat{f}_C(k) - \hat{f}(k) \right| \left(\frac{2}{\pi k} \right)^\lambda (l+\lambda) J_{l+\lambda}(\pi k). \end{aligned}$$

where we used Eq.(2.13) in the first step, the collocation analogies of Eqs.(2.5), (2.2) in the second and third steps, and Eq.(2.14) in the last step.

We can continue the estimates for the collocation error by using Eq.(2.13) and the property $|J_\nu(x)| \le 1$ for all $x,\ \nu \ge 0$ ([9], page 362):

$$
\begin{aligned}
|\, CE(x,\lambda,m,N)\,| \;&\le\; \sum_{l=0}^{m} \frac{\Gamma(l+2\lambda)\Gamma(\lambda)(l+\lambda)}{l!\Gamma(2\lambda)} \sum_{|k|\le N} \left|\hat{f}_C(k)-\hat{f}(k)\right| \left(\frac{2}{\pi k}\right)^{\lambda} J_{l+\lambda}(\pi k) \\
&\le\; \frac{\Gamma(m+2\lambda)\Gamma(\lambda)(m+\lambda)}{(m-1)!\Gamma(2\lambda)} \sum_{|k|\le N} \left|\hat{f}_C(k)-\hat{f}(k)\right| \left(\frac{2}{\pi k}\right)^{\lambda} J_{l+\lambda}(\pi k) \qquad (4.2a) \\
&\le\; \frac{\Gamma(m+2\lambda)\Gamma(\lambda)(m+\lambda)}{(m-1)!\Gamma(2\lambda)} \left(\frac{2}{\pi}\right)^{\lambda} \left|\hat{f}_C(k)-\hat{f}(k)\right| \\
&\le\; A(m,\lambda)\, \left|\hat{f}_C(k)-\hat{f}(k)\right|_{max} . \qquad (4.2b)
\end{aligned}
$$

Here we also used the fact that $\frac{(l+\lambda)\Gamma(l+\lambda)}{l!}$ is an increasing function of l.

The maximum difference $\delta(N) = |\hat{f}_C(k) - \hat{f}(k)|_{max},\ |k| \le N$ between the exact and the approximated values of the Fourier coefficients decreases as N becomes larger. Typically, $\delta(N) \sim 10^{-3} - 10^{-4}$ for $N \sim 10^2 - 10^3$. As for the coefficient $A(m,\lambda)$ in Eq.(4.2b), it increases rapidly with m and λ, so that $A(5,5) \sim 10^5,\ A(10,10) \sim 10^{13}$ and so on. Therefore, one could expect that even small deviations of $\hat{f}(k)$ from their exact values will produce a large error in the FG approximation.

However, the numerical experiments show that the accuracy is *almost the same* for the Galerkin and the collocated FG methods if N is large enough. Table 1 gives the maximum error of the FG approximation in the case $f(x) = \sin \frac{1}{2}\pi x,\ \ x \in [-1,1]$.

At low resolutions the accuracy even better, by chance, for the collocation method.

N	32	48	64
Galerkin	5.0 (-5)	1.2 (-8)	1.7 (-11)
collocation	1.6 (-6)	1.8 (-9)	4.9 (-10)

Table 1: The accuracy of the Galerkin and the collocated FG methods for the function $f(x) = \sin \frac{1}{2}\pi x, \quad \lambda = 20, m = 16.$

It turns out, unexpectedly, that the high accuracy of the collocation method is due to the fact that the summation of k of (2.6) converges precisely to the same limit value for both $\hat{f}(k)$ and $\hat{f}_C(k)$, as shown in Fig. 2. Evidently, the collocation error CE becomes smaller due to the bound in Eq.(4.2a) (but not in Eq.(4.2b)). The proof of this fact will be reported separately.

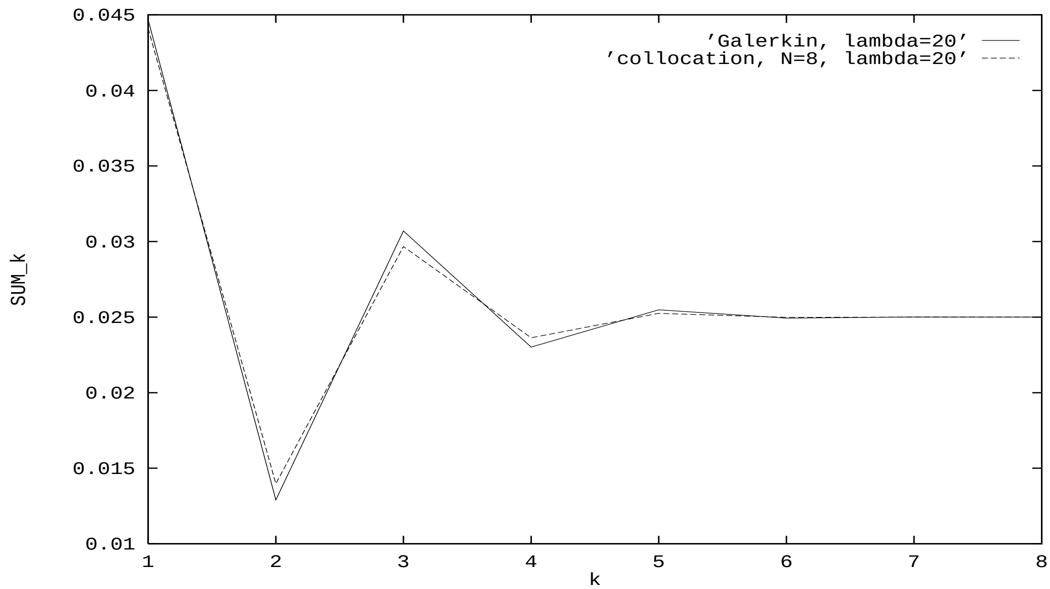

Figure 2: Convergence of the summation on k in Eq. (2.6) using the Galerkin and the approximated (collocation) Fourier Coefficients

5 Analysis of the Regularization Error: Moderate m

In this section we analyze the convergence of the Gegenbauer series for moderate m (the number of terms in the expansion (Eq. (2.7)). The analysis is performed for the wave function Eq.(3.8). The Gegenbauer coefficients (Eq.(2.6)) of this function are expressed as:

$$\hat{f}^{\lambda}(l) = \Gamma(\lambda) i^{l} (l+\lambda) J_{l+\lambda}(\pi\omega) \left(\frac{2}{\pi\omega}\right)^{\lambda} \hat{f}(\omega) \tag{5.1}$$

(see [10], page 213).

Let us denote the magnitude of the lth term in the Gegenbauer expansion by

$$T_l = \max_{-1 \le x \le 1} \left| \hat{f}^{\lambda}(l) C_l^{\lambda}(x) \right| \tag{5.2}$$

where the dependence on ω and λ is suppressed on the LHS for simplicity of notation. Using (5.2) and the relations (2.13) we get:

$$T_l = \mid f^{\lambda}(l) \mid \cdot \mid C_l^{\lambda}(1) \mid$$

$$= \frac{\Gamma(l+2\lambda)\Gamma(\lambda)}{l!\Gamma(2\lambda)}(l+\lambda) \mid J_{l+\lambda}(\pi\omega) \mid \left(\frac{2}{\pi\omega}\right)^{\lambda} \tag{5.3}$$

Figs. 3 and 4 show the magnitude of the terms T_l for several ω and λ. The quantities T_l first grow with l until a maximum is reached at $l = \mu$ where μ satisfies

$$T_\mu = \max_{0<l<\infty} T_l. \tag{5.4}$$

Then, for $l > \mu$ these terms decay (obviously we can expect convergence of the Gegenbauer series only in this region). μ itself is a growing function of ω for fixed λ, which means that more terms are needed for convergence at larger ω.

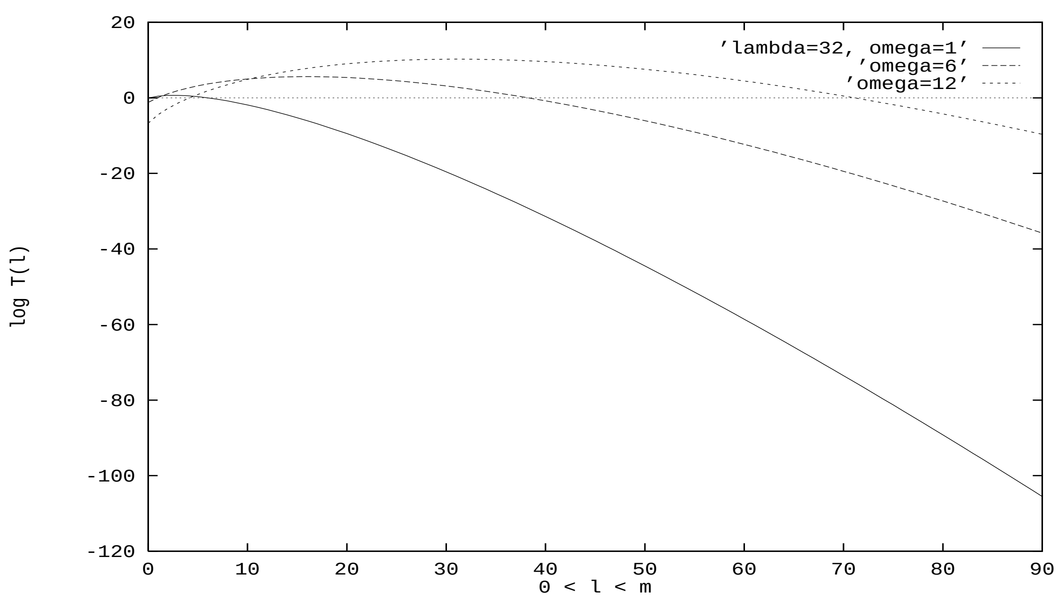

Figure 3: Magnitude of the Gegenbaur terms $T_l(1)$

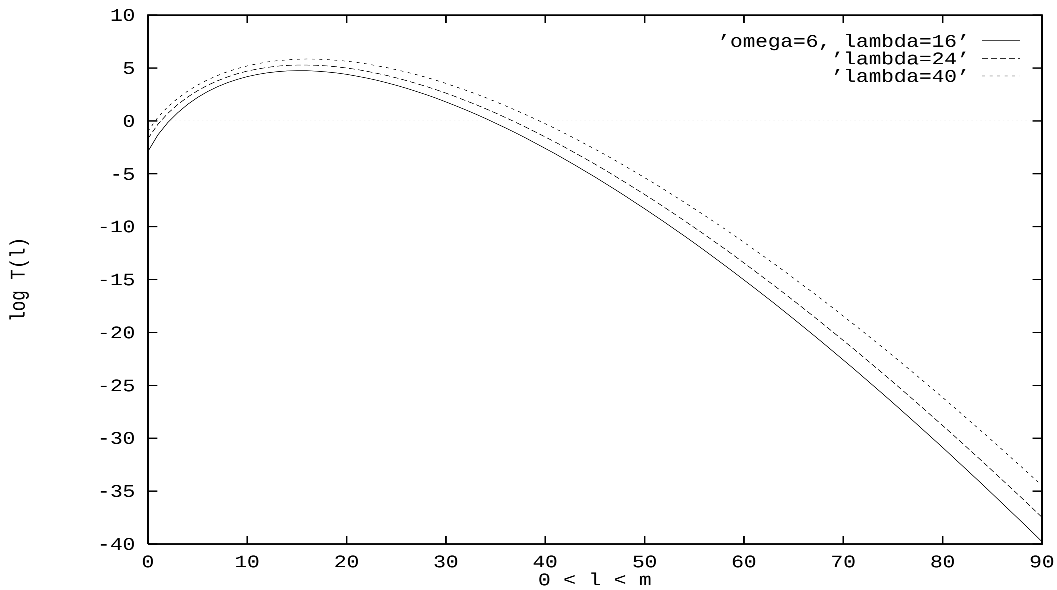

Figure 4: Influence of λ on the magnitude of the Gegenbaur terms

To estimate μ, we consider the ratio r_l:

$$\begin{aligned} r_l &\equiv \frac{T_{l+1}}{T_l} \\ &= \frac{\Gamma(l+2\lambda+1)}{\Gamma(l+2\lambda)}\ \frac{\Gamma(l+1)}{\Gamma(l+2)}\ \frac{l+\lambda+1}{l+\lambda}\ \frac{J_{l+\lambda+1}(\pi\omega)}{J_{l+\lambda}(\pi\omega)} \\ &= \frac{(l+2\lambda)(l+\lambda+1)}{(l+\lambda)(l+1)}\ \frac{J_{l+\lambda+1}(\pi\omega)}{J_{l+\lambda}(\pi\omega)} \end{aligned} \tag{5.5}$$

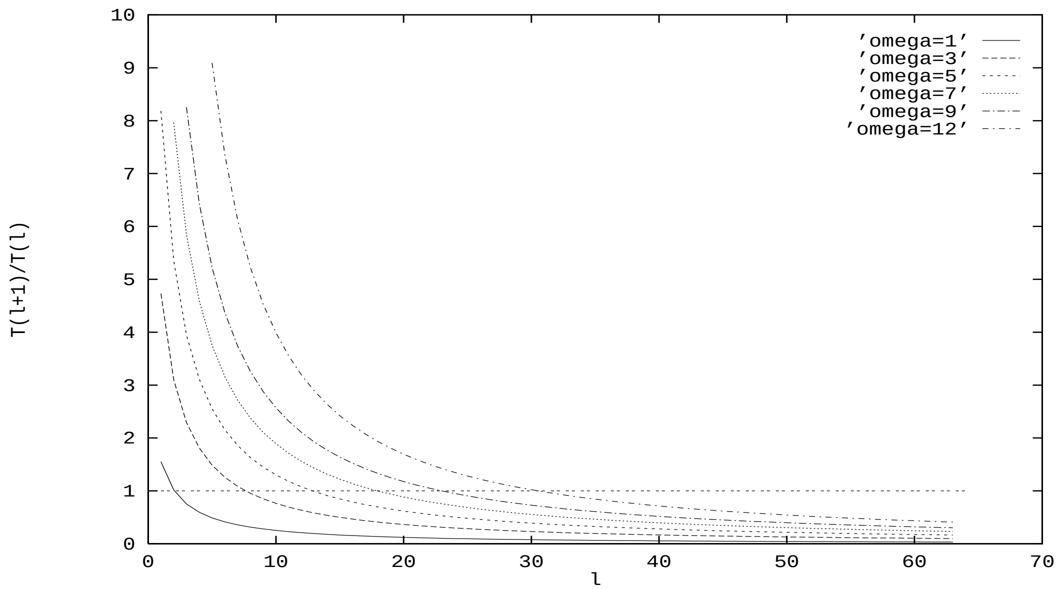

Figure 5: Intersection of a curve $w = const$ with the horizontal line $\frac{T_{l+1}}{T_l} = 1$ gives the number $l = \mu(\omega)$ of the largest term T_μ

Fig. 5 shows several graphs r_l as a function of l for different ω. The points of intersection with the line $r = 1$ correspond to maximum values of T_l so that the relation

$$r_\mu = 1 \tag{5.6}$$

could be used to compute μ. It is also true that $T_{\mu-1} \approx T_{\mu+1}$ which implies

$$r_\mu r_{\mu-1} \approx 1. \tag{5.7}$$

Combining (5.5)-(5.7) we obtain a much simpler relation between μ, ω and λ which does not contain Bessel functions. Let

$$\varphi(\mu, \lambda) = \frac{(\mu + 2\lambda)(\mu + 2\lambda - 1)(\mu + \lambda + 1)}{\mu(\mu + 1)(\mu + \lambda - 1)}$$

then we have

$$r_\mu r_{\mu-1} =$$

$$= \varphi(\mu, \lambda) \; \frac{J_{\mu+\lambda+1}(\pi\omega)}{J_{\mu+\lambda-1}(\pi\omega)} \tag{5.8}$$

$$= \varphi(\mu, \lambda) \; \left(\frac{\mu + \lambda}{\pi\omega/2} \, \frac{J_{\mu+\lambda}(\pi\omega)}{J_{\mu+\lambda-1}(\pi\omega)} - 1 \right) \tag{5.9}$$

$$= \varphi(\mu, \lambda) \; \left(\frac{r_{\mu-1}}{\pi\omega/2} \, \frac{\mu(\mu + \lambda - 1)}{\mu + 2\lambda - 1} - 1 \right) \tag{5.10}$$

$$\approx \varphi(\mu, \lambda) \; \left(\frac{2}{\pi\omega} \, \frac{\mu(\mu + \lambda - 1)}{\mu + 2\lambda - 1} - 1 \right) . \tag{5.11}$$

We used the relation $J_{n+1}(x) + J_{n-1}(x) = (2n/x)J_n(x)$ in (5.9), expression (5.5) in (5.10) and the estimates (5.6), (5.7) in (5.11).

With more simplifications we get the following relation:

$$\frac{2}{\pi\omega} \approx \frac{\mu + 1}{(\mu + 1 + \lambda)(\mu + 2\lambda)} + \frac{\mu + 2\lambda - 1}{\mu(\mu + \lambda - 1)}. \tag{5.12}$$

If we denote $\gamma = \lambda/\mu$ and assume that $\mu \gg 1$ we can simplify (5.12) to be

$$\mu \approx \beta(\gamma)\pi\omega, \qquad\qquad \beta(\gamma) = \frac{1 + 2\gamma + 2\gamma^2}{1 + 3\gamma + 2\gamma^2} \tag{5.13}$$

(actually this estimate is fairly accurate already for $\mu > 5 - 10$). Evidently, for all γ $\beta(\gamma) < 1$. It tends to unity for $\gamma \gg 1$ or $\gamma \ll 1$, and has a broad minimum at $\gamma = 1/\sqrt{2}$ where it approaches the value $\beta_{min} \approx 0.83$, i.e.

$$0.83 < \beta(\gamma) < 1. \tag{5.14}$$

We conclude that μ depends only slightly on λ.

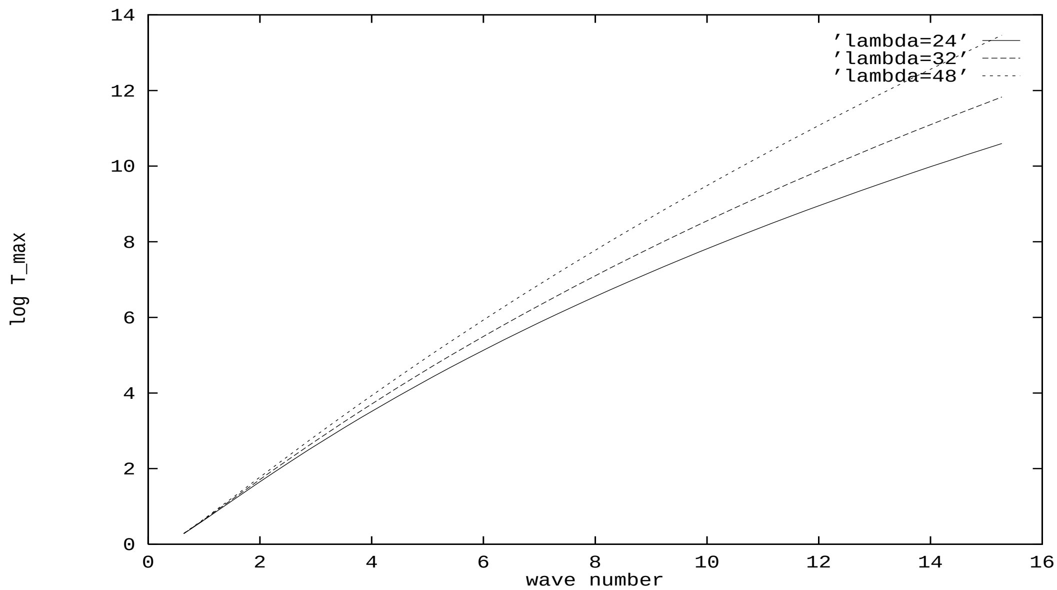

Figure 6: Growth of the largest term T_{mu} with the wave number ω

The dependence of the largest term T_μ as a function of ω is shown in Fig. 6 for several values of λ. It can be proved that $T_\mu \propto e^{\pi\omega}$ for $\pi\omega \ll \lambda$ and $T_\mu \propto 2^\mu \approx e^{0.58\pi\omega}$ for $\pi\omega \sim \lambda$. Therefore, the largest term in the Gegenbauer expansion *grows exponentially* with ω.

We have shown that for the wave function (3.8) the Gegenbauer series does not converge monotonically. The index μ of the largest term in the series increases in proportion to ω, and its amplitude T_μ grows exponentially. This result, however, does not contradict the fact that the Gegenbauer series converges exponentially with m if $m = \beta\pi\omega$, where β satisfies the conditions of (3.9). If, for example, $\lambda/m = 1$ and we increase both m and ω so that $m = \beta\omega$, we will get an exponentially *growing* sequence of terms T_m for $\beta = \frac{5}{6} \approx 0.83$, and exponentially *decreasing* sequence of terms for $\beta \approx 7/\pi \approx 2.2$.

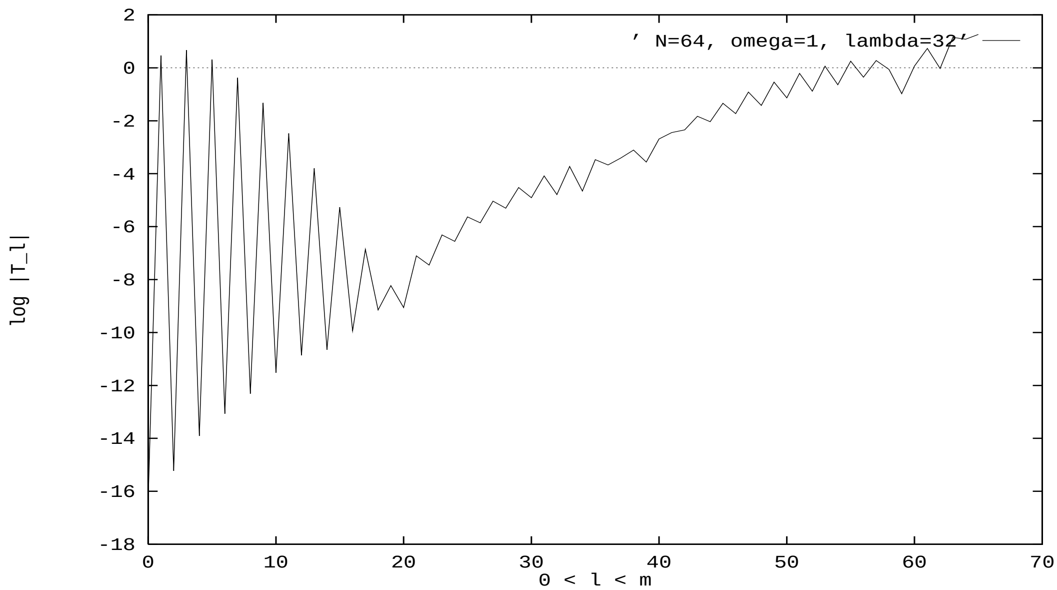

Figure 7: Amplification of the Gegenbaur terms ($l > 20$) due to the presence of computational "noise", generated by the collocation procedure with $N = 64$ modes

The rapid amplification of the Gegenbauer terms in the series for waves with high frequency should be taken into account when a pseudospectral version of the FG method is employed. We illustrate the difficulties on a simple example $f(x) = \sin \pi x$. Fig. 7 displays the magnitude of the terms $T_l(1)$ as a function of l for $N = 64, \lambda = 32$. Compare this graph with the corresponding curve at $\omega = 1$ in Fig. 3 obtained with the exact Fourier coefficients in Eq.(2.6). Notice that the "sawtooth" shape in Fig. 7 is due to the fact that $f(x) = \sin \pi x$ is a real antisymmetric function, whose Gegenbauer expansion must contain only odd terms $l = 1, 3, ...$, while the smoothness in Fig. 3 is related to the complex wave function Eq.(3.8). The Gegenbauer terms in Fig. 3 decrease monotonically for $l > \mu \approx \pi$, whereas in the pseudospectral case they decrease only until $l \approx 20$ where $T_{20} \sim 10^{-9}$, then for $l > 20$ these terms grow rapidly, destroying the convergence.

The explanation for this surprising behavior is the following. The vector of exact Fourier coefficients $\hat{f}_k$, used in the spectral method, contains only non-zero components $\hat{f}_{\pm 1} = \mp \frac{i}{2}$. In the pseudospectral method, the numerical computation of the Fourier coefficients by using the DFFT introduces round-off errors and, instead of zeros, we have $\hat{f}_k \sim 10^{-16}$ for $1 < |k| \leq N$. According to the above consideration, the presence of rapidly oscillating components in $\hat{f}_k$ with large $k \sim N$ leads to amplification of "false" terms in (2.6), destroying completely the accuracy.

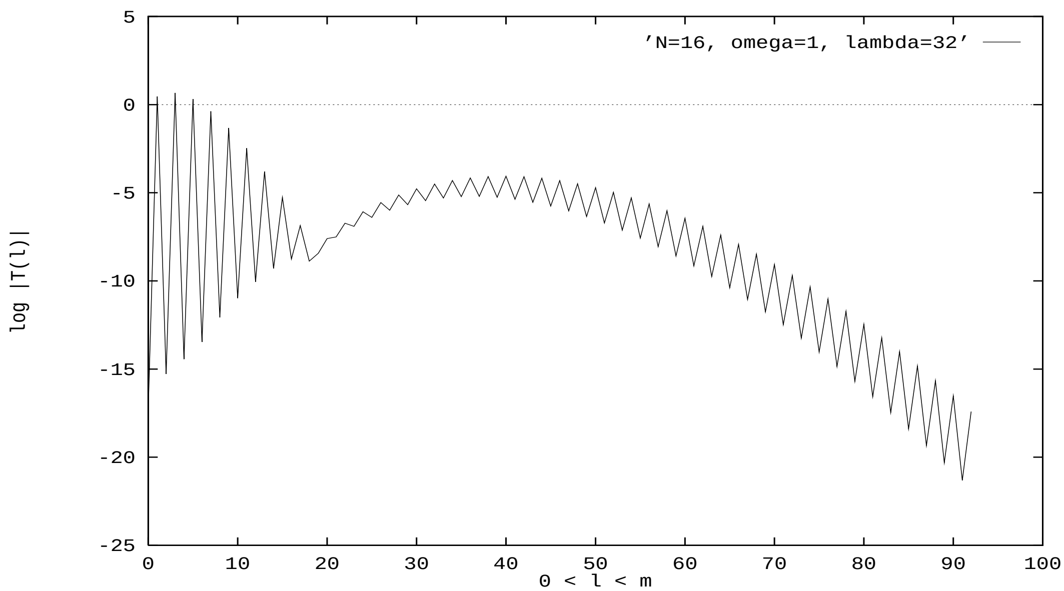

Figure 8: Amplification of ($l > 20$) and decay ($l > 40$) of the Gegenbauer terms in the collocation procedure with $N = 16$ modes

The behavior of the Gegenbauer terms in the case $N = 16, \lambda = 32$ is shown in Fig. 8. Initially, $T_l(1)$ decreases until $l \approx 20$. Then, for $l > 20$ the growing of "false" terms overtake the "right" terms, breaking up the accuracy. When l increases more, T_l reaches the maximum slope at $l \approx 40$ (according to estimate (4.14) at $\omega = N = 16$) and, ultimately, decay in the region $l > \mu$. The amplification factor $|T_\mu|/|T_0| \sim 10^{-4}/10^{-16} \sim 10^{12}$ is in accordance with the corresponding curve in Fig. 6 for $\lambda = 32, k = 16$. Note that the maximum slope in Fig. 7 ($N = 64$) is expected at $l \approx 166$.

To conclude, the *collocated* FG method fails when applied to rapidly oscillating functions (or, more generally, to functions having steep profiles with large gradients). The major factor which causes the loss of accuracy is the fast amplification of short wave components in the computational "noise" (arising due to cut-off errors) with spatial frequencies $\omega \approx N$, where $2N + 1$ is the number of collocation points. Nevertheless, this method is still very accurate (in fact, spectrally accurate) for smooth functions. We call the function "smooth" if it can be represented accurately by a small number of terms in the Gegenbauer expansion (in this sense functions $f(x) = x$ or $f(x) = \sin 1.4x$ are very smooth). In such case, the Gegenbauer series converges fast enough to give a spectrally accurate approximation before the "noise" has grown up considerably. This observation shows us the way how to modify the current FG method in order to treat correctly and accurately functions with steep profiles. This is described in the next section.

6 Computation of Local Quantities

Suppose we are given for an analytic (or piecewise analytic) function $f(x)$ on the interval $x \in [-1,1]$ the values $f(x_i)$, $i = 1, 2, ..., 2N+1$. We are interested in computing the values (or gradients) of $f(x)$ at some particular locations $x = x_p$. In such a case we can apply the FG method on a smaller sub-interval $[a,b] \subset [-1,1]$ in the vicinity of the point of interest. Furthermore, if the function $f(x)$ has a "rough" profile, we expect that a local FG approximation to be more accurate than the global one (constructed on the whole interval $-1 \le x \le 1$) provided that $f(x)$ is smooth enough in $a \le x \le b$ and that the the local resolution is sufficiently large.

Let us define a sub-interval $[a,b] \subset [-1,1]$ and introduce the local variable ξ

$$x(\xi) = \xi l + \bar{x}$$

$$l = \frac{b-a}{2}, \quad \bar{x} = \frac{b+a}{2} \tag{6.1}$$

such that $a \le x \le b$ when $-1 \le \xi \le 1$. The number of collocation points in $[a,b]$ is $2n+1$, where $n = N\ l$ and $l \le 1$ ($l = 1$ corresponds to the case $[a,b] = [-1,1]$).

We construct, initially, the Fourier partial sum on a sub-interval $x \in [a,b]$:

$$f_n(x(\xi)) = \sum_{k=-n}^{n} \hat{f}(k) e^{ik\pi\xi}, \qquad \xi \in [-1,1] \tag{6.2}$$

where

$$\hat{f}(k) = \frac{1}{2} \int_{-1}^{1} f(x(\xi)) e^{-ik\pi\xi} d\xi, \qquad |k| \le n \tag{6.3}$$

The Gegenbauer expansion of $f(x)$ on the sub-interval $[a,b]$ is

$$f(x(\xi)) = \sum_{l=0}^{\infty} \hat{f}^{\lambda}(l) C_l^{\lambda}(\xi) \tag{6.4}$$

where the Gegenbauer coefficients $\hat{f}^{\lambda}(l)$ are given by

$$\hat{f}^{\lambda}(l) = \frac{1}{h_l^{\lambda}} \int_{-1}^{1} (1-\xi^2)^{\lambda-\frac{1}{2}} f(x(\xi)) C_l^{\lambda}(\xi) d\xi \tag{6.5}$$

Assume, as before, that we do not have $f(x)$ at our disposal but only its approximation (6.2). Thus, we have

$$\hat{g}_n^{\lambda}(l) = \frac{1}{h_l^{\lambda}} \int_{-1}^{1} (1-\xi^2)^{\lambda-\frac{1}{2}} f_n(x(\xi)) C_l^{\lambda}(\xi) d\xi \tag{6.6}$$

Then, the corresponding *local* Fourier-Gegenbauer expansion of $f(x)$ on the sub-interval $[a, b]$ is

$$f_{m,n}^{\lambda}(x(\xi)) = \sum_{l=0}^{m} \hat{g}_n^{\lambda}(l) C_l^{\lambda}(\xi). \tag{6.7}$$

If $f(x)$ is smooth on $[a, b]$ and the number of collocation points in $[a, b]$ is large enough then, according to section 4, the accuracy of the local FG approximation is as good as desired.

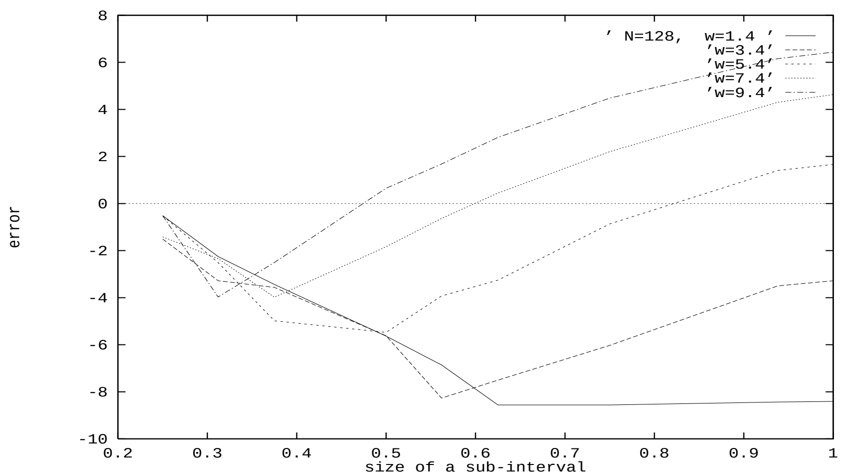

Figure 9: The error of the local FG approximation in the case $f(x) = \sin \omega\pi x$

We demonstrate the precision of the local FG approach for the case $f(x) = \sin \omega\pi x,\ x \in [-1, 1]$. Fig. 9 shows the maximum approximation error $\varepsilon(f) = \max_{x\in[a,b]} |f_{m,n}^{\lambda}(x) - f(x)|$ as a function of $l = (b-a)/2$ for $N = 128,\ m = 25,\ \lambda = 16,\ \bar{x} = -1+l$ (the sub-interval $[a, b]$ is located near the left boundary). The error decays while l is reduced to $l_*(\omega) < l < 1$ because $f(x)$ appears "smoother" on a smaller sub-interval. For $l < l_*(\omega)$ the error grows rapidly because the number of collocation points in $[a, b]$ becomes too small to ensure a sufficient resolution. The optimal size of $l_*(\omega)$ results from the competition between two factors: the local resolution which is proportional to l, and the "smoothness" of a local profile which requires a smaller l. The minimal error $\epsilon(l_*)$ is a growing function of ω. However, the accuracy of the local FG approximation can be improved by increasing the resolution -see Fig. 10 for $\omega = 5.4$; $N = 128$ and $N = 256$ ($l_* \approx 0.4$).

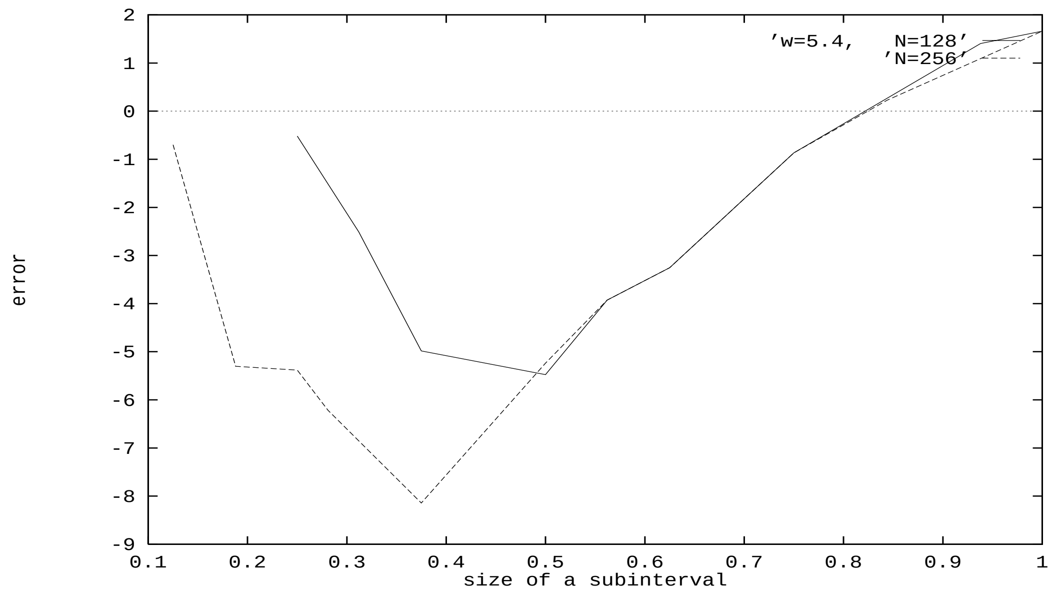

Figure 10: Improvement of accuracy by increasing resolution

Another example is given in Table 2 which demonstrates the ability of the local FG method to resolve a large gradient near the boundaries: $f(x) = \sinh\ \alpha x/\sinh\ \alpha$. The computational interval $x \in [a, b]$ is of a size $2l$ and is adjacent to the left boundary. The parameters are $N = 64, m = \lambda = 16$.

α	$2l$	$\varepsilon(f)$	$\varepsilon(f')$	$\varepsilon(f'')$
	1/2	1.2 (-5)	1.2 (-5)	1.2 (-5)
20	1/3	5.6 (-9)	1.5 (-8)	3.3 (-7)
	1/5	9.4 (-11)	3.3 (-8)	9.0 (-7)

Table 2: The accuracy of the local FG method for the function $f(x) = \sinh \alpha x/\sinh \alpha$; the variable computational interval $2l$ adjoins the boundary $x = -1$

The error reduces with the size $2l$. Note that due to similarity of the function $f = \sinh \alpha x/\sinh \alpha$ the same accuracy can be obtained for *any* big α provided that $l \propto 1/\alpha$ and the resolution on the sub-interval $2l$ remains unchanged.

Some remarks:

1. Since the local FG method operates with the Fourier coefficients computed on a sub-

interval $[a,b] \subset [-1,1]$ (Eq. (6.3)), only part of the available information, the values of $f(x)$ on the whole interval, is utilized. Nevertheless, the local FG approximation is more accurate than the global one for rough distributions, provided that the local resolution is sufficiently large.

2. For rapidly oscillating or shock-like functions with large local gradients, a spectrally accurate approximation can be constructed on the whole interval as a direct sum of appropriate local approximations. We split the interval of interest into pieces such that the function is smooth within each of these pieces, and apply the local FG algorithm on every sub-interval as it is described in this section. The same approach can be realized for a discontinuous but piecewise analytic function.

3. Unlike pseudospectral Fourier methods which require uniform resolution, the present FG algorithm allows us to use variable (non-uniform) resolution for different parts of the domain. This leads us to the possibility using it for treating unstructured grids.

4. Another local Fourier-Gegenbauer approach is described in [3]. This approach deals with the re-expansion of the Fourier partial sums, computed globally, into local Gegenbauer series. The comparison between these local techniques will be discussed in a future paper.

7 Hybrid Fourier-Gegenbauer (HFG) method

The ability of the FG method to evaluate precisely the derivatives of a non-periodic function on the boundaries, can be employed to construct a high order spectral algorithm for the solution of non-periodic differential equations. The algorithm incorporates the pseudospectral Fourier (PSF) method. The FG technique allows us to remove, to a great extent, the discontinuity on the boundaries in order to accelerate the convergence of the Fourier series in the PSF method.

The Fourier series for a function $f(x)$ converges rapidly if the function and a certain number of its first derivatives are continuous and periodic. Namely, for a C^m- function (such that $f(x), f'(x), ..., f^{(m)}$ are continuous and periodic) the Fourier series converges as $O(N^{-(m+1)})$. If, in addition, f^{m+1} has a bounded variation, the series converges as $O(N^{-(m+2)})$- see [11].

For a smooth but non-periodic function, having discontinuous periodic extension, the Fourier series converges very slowly like $O(N^{-1})$. To accelerate the rate of convergence one can employ a polynomial subtraction technique [12] (which is also known as the method of Krylov [13]). It consists of removing from the given function a polynomial which has the same discontinuities and such that its several first derivatives have the same discontinuities. To implement this one should know the derivatives of the function on the boundaries. The FG method enables us to evaluate, within spectral accuracy, the derivatives on the boundaries.

Our *Hybrid Fourier-Gegenbauer* (HFG) method is demonstrated on the 1D modified Helmholtz equation with Dirichlet type boundary conditions

$$\mathcal{L}(\mu)U \equiv \frac{d^2U}{dx^2} - \mu^2 U = f(x), \quad x \in [-L, L]$$

$$U(-L) = G_-, \ \ U(L) = G_+ \tag{7.1}$$

Here, $f(x)$ is a C^∞- function in $x \in [-L, L]$, μ is a constant parameter. The computational algorithm consists of the following steps:

1. *Computation of f'', f^{IV} on the boundaries.*
   We define two "small" sub-intervals $[-L, -L+2l]$, $[L-2l, L]$, adjacent to the boundaries $x = \pm L$, such that the function $f(x(\xi))$ is smooth on the scale of $\xi = (x \pm L)/l \mp 1$, $\xi \in (-1, 1)$. On each of these sub-intervals we apply the local FG algorithm (see section 5) to compute on the boundaries the derivatives f'', f^{IV} of the source function $f(x)$.

2. *Smoothing of the source function.*
   We "extract" the smooth part $f_s(x)$ from the function $f(x)$ by using a polynomial subtraction technique:

$$f(x) = f_s(x) + \sigma_s(x), \qquad x \in [-L, L]$$
$$\sigma_s(x) = \sum_{n=0}^{s} a_n x^n. \tag{7.2}$$

   The polynomial σ_s has to be such that f_s and its several even derivatives vanish on the boundaries. For instance, for $s = 1, 2, 3$ we have

$$\begin{aligned} s &= 1, \qquad & f_s(\pm L) &= 0, \\ s &= 2, \qquad & f_s(\pm L) &= f_s''(\pm L) = 0, \\ s &= 3, \qquad & f_s(\pm L) &= f_s''(\pm L) = f_s^{IV}(\pm L) = 0 \end{aligned} \tag{7.3}$$

   The coefficients a_n can be expressed in terms of the boundary values $f(\pm L)$, $f''(\pm L)$, $f^{IV}(\pm L)$, computed in the previous step. We define

$$L^{-n} f_+^{(n)} = \frac{f^{(n)}(1) + f^{(n)}(-1)}{2}, \qquad L^{-n} f_-^{(n)} = \frac{f^{(n)}(1) - f^{(n)}(-1)}{2}; \qquad n = 0, 2, 4$$

   and for $s = 3$

$$\begin{aligned} a_0 &= f_+ - \tfrac{1}{2} f_+'' + \tfrac{5}{24} f_+^{IV} \qquad & L a_1 &= f_- - \tfrac{1}{6} f_-'' + \tfrac{7}{360} f_-^{IV} \\ L^2 a_2 &= \tfrac{1}{2} f_+'' - \tfrac{1}{4} f_+^{IV} \qquad & L^3 a_3 &= \tfrac{1}{6} f_-'' - \tfrac{1}{36} f_-^{IV} \\ L^4 a_4 &= \tfrac{1}{24} f_+^{IV} \qquad & L^5 a_5 &= \tfrac{1}{120} f_-^{IV} \end{aligned} \tag{7.4}$$

   (for $s = 2$ we should omit in (7.4) the terms with the fourth derivative and for $s = 1$ we omit the terms with the second and the fourth derivatives).

After antisymmetric extension into the interval $(L, 3L)$ we get a $C^{(2s-1)}$-function $\tilde{f}_s(x)$

$$\tilde{f}_s(x) = \begin{cases} f_s(x), & -L < x < L, \\ -f_s(2L - x), & L < x < 3L \end{cases} \tag{7.5}$$

This function can be represented by the Fourier series which converges at least as $O(N^{-2s})$ (or even faster, depending on whether or not the derivative f^{VI} is bounded on the interval $[-L, L]$).

3. *Construction of the particular solution.*
We find a particular solution $U_p(x)$ for the problem (7.1) with any (unspecified) boundary conditions. U_p is represented as a superposition of two solutions according to the partition of the source function (7.2):

$$U_p = \tilde{U}_p^{(s)} + U_\sigma^{(s)} \tag{7.6}$$

where $\tilde{U}_p^{(s)}$ and $U_\sigma^{(s)}$ satisfy

$$\mathcal{L}(\mu)\tilde{U}_p^{(s)} = \tilde{f}_s(x), \quad x \in [-L, 3L] \tag{7.7}$$

$$\mathcal{L}(\mu)\tilde{U}_\sigma^{(s)} = \sigma_s(x), \quad x \in [-L, L] \tag{7.8}$$

Eq. (7.7), with the smooth source function $\tilde{f}_s$ in the RHS, is solved by using the PSF method on the extended interval $[-L, 3L]$:

$$\begin{array}{lcl} \tilde{f}_s(x) & \xrightarrow{\text{FFT}} & \hat{f}_k^{(s)}, \\ \hat{U}_k^{(s)} & = & -\quad \hat{f}_k^{(s)}/(k^2 + \mu^2), \\ \hat{U}_k^{(s)} & \xrightarrow{\text{FFT}} & \tilde{U}_p^{(s)}(x) \end{array}$$

Eq. (7.8) is integrated explicitly. The solution has the same polynomial form $U_\sigma^{(s)} = \sum_{n=0}^{s} b_n x^n$ as that of the source function $\sigma_s(x)$. The coefficients b_n can be easily derived from the terms of a_n and μ.

4. *Correction for the true boundary conditions.*
The solution of the original problem (7.1) with the prescribed boundary conditions in $x = \pm L$ is obtained by combining the particular solution U_p (below we omit the superscript "s") with two independent solutions $H_{1,2}(x)$ of the corresponding homogeneous problem as follows:

$$\mathcal{L}(\mu)H_{1,2} = 0, \quad x \in [-L, L] \tag{7.9}$$

$$U(x) = U_p(x) + AH_1(x) + BH_2(x), \tag{7.10}$$

Assume $\mu =$ constant, then the solutions for (7.9) can be written explicitly in the form

$$H_1 = e^{\mu(x-L)}, \ H_2 = e^{-\mu(x+L)}$$

The constant coefficients $A,\ B$ are derived from the boundary conditions $U(\pm L) = G_\pm$:

$$A = \frac{G_+ - U_p(L) - e^{-2\mu L}(G_- - U_p(-L))}{1 - e^{-4\mu L}},$$

$$B = \frac{G_- - U_p(-L) - e^{-2\mu L}(G_+ - U_p(L))}{1 - e^{-4\mu L}}.$$

We demonstrate the precision of the HFG method on some typical examples. Table 3 shows the maximum numerical error $\varepsilon_s,\ s = 1,2,3$ for a solution $u = x^n,\ 4 \le n \le 24,\ \ x \in [-1,1]$; the source function $f(x)$ in (7.1) is chosen accordingly, s denotes the degree of the subtraction polynomial in (7.2). The computational parameters are: $L = 1, \mu = 10, N = 64$.

n	ε_1	ε_2	ε_3	ε_{FG}
4	3.1 (-7)	7.4 (-12)	3.0 (-15)	5.2 (-10)
9	1.1 (-6)	7.5 (-10)	3.6 (-13)	1.9 (-10)
14	1.5 (-6)	7.4 (-10)	9.3 (-13)	3.4 (-9)
19	1.7 (-5)	3.1 (-8)	2.4 (-11)	9.8 (-9)
24	5.2 (-5)	2.2 (-7)	7.9 (-10)	3.5 (-2)

Table 3: The numerical error of the HFG ($\varepsilon_s,\ \ s = 1,2,3$) and the FG ($\varepsilon_{FG}$) methods for the solution $u = x^n$.

Naturally, the error decays as the degree of smoothness s increases. The precision remains very high up to steep distributions near the boundaries ($n = 24$). The last column in Table 3 gives the error for the solution that is computed by the "pure" FG method with the same resolution ($N = 64, m = \lambda = 20$). For $n = 24$ the error jumps up because the basic functions in the Gegenbauer expansion (2.3) with $m = 20$ terms do not contain a polynomial of the required order $n = 24$. The accuracy of the HFG method with $s = 3$ is several order of magnitude higher in comparison to the FG method. This conclusion remains valid for every μ.

Another example is the solution $u = 0.5(1 + \tanh\ \alpha x),\ x \in [-1,1]$ which exhibits steep distribution in the vicinity of $x = 0$. This case is especially favorable for the FGH method since the source function is smooth near the boundaries, where the FG technique is employed. The results are shown in Table 4 for $\mu = 10$ and several values of α and N.

The precision of the HFG algorithm in this case is much higher than that of the FG method (the last column, $m = \lambda = 16$). For $\alpha = 20$ the accuracy does not depend on the degree of smoothness s on the boundaries because it is limited by the resolution of the inner shock. An important fact, indicating a good convergence, is that the accuracy substantially improves (by four order of magnitude) as N is doubled (compare results for $N = 32$ and $N = 64$ at $\alpha = 20$).

The following example deals with the solution $u = \sinh \alpha x / \sinh \alpha,\ x \in [-1,1]$. Such a case is the most challenging for the HFG method since the steepest distribution takes place near the boundaries where the FG method is applied. The results are shown in Table 5 for $\mu = 10$. High accuracy is preserved even for very steep distributions ($\alpha = 20$).

N	α	ε_1	ε_2	ε_3	ε_{FG}
32	1	1.2 (-7)	5.8 (-11)	8.6 (-11)	3.8 (-6)
	5	8.9 (-13)	1.4 (-10)	5.2 (-10)	7.5 (+1)
	10	1.8 (-8)	1.8 (-8)	1.8 (-8)	1.6 (+3)
	20	2.1 (-4)	2.1 (-4)	2.1 (-4)	6.0 (+3)
64	1	8.5 (-9)	4.4 (-12)	4.9 (-12)	1.9 (-6)
	5	6.1 (-14)	1.0 (-11)	1.7 (-11)	7.5 (+1)
	10	9.6 (-14)	1.3 (-12)	3.9 (-12)	1.6 (+3)
	20	1.9 (-8)	1.9 (-8)	1.9 (-8)	6.0 (+3)

Table 4: The accuracy of the HFG and FG algorithms for the shock-like solution $u = 0.5(1 + \tanh\ \alpha x)$

N	α	ε_1	ε_2	ε_3	ε_{FG}
64	1	2.6 (-8))	3.0 (-13)	5.5 (-16)	4.3 (-11)
	5	4.9 (-7)	1.4 (-10)	4.0 (-14)	7.4 (-7)
	10	2.6 (-6)	3.2 (-9)	1.6 (-13)	1.2 (-3)
	20	3.1 (-5)	1.4 (-7)	6.7 (-10)	1.1 (-1)

Table 5: The accuracy of the HFG and the FG algorithms for the solution $u = \frac{\sinh\ \alpha x}{\sinh\ \alpha}$

The last example is the wave function $u = \sin \omega\pi x,\ x \in [-1, 1]$. The results are presented in Table 6 for $\mu = 10$. We can see again that the precision and resolution properties of the

N	ω	ε_1	ε_2	ε_3	ε_{FG}
32	1.4	8.1 (-6)	7.5 (-9)	9.7 (-12)	1.0 (-5)
	3.4	8.6 (-5)	4.7 (-7)	2.5 (-9)	6.1 (0)
	6.4	7.9 (-4)	1.4 (-5)	2.6 (-7)	1.8 (+4)
64	1.4	5.7 (-7)	1.3 (-10)	2.7 (-14)	2.8 (-8)
	3.4	6.1 (-6)	8.2 (-9)	1.2 (-11)	1.1 (-2)
	6.4	5.1 (-5)	2.4 (-7)	1.1 (-9)	1.5 (+4)
128	1.4	3.7 (-8)	2.1 (-12)	2.7 (-14)	2.8 (-8)
	3.4	4.0 (-7)	1.3 (-10)	2.1 (-12)	1.1 (-2)
	6.4	3.4 (-6)	4.0 (-9)	7.6 (-11)	1.5 (+4)

Table 6: The accuracy of the HFG and the FG methods for the oscillatory solution $u = \sin\ \omega\pi x$

HFG method are much better than those of the FG method.

Conclusion

The efficient implementation of the Fourier-Gegenbauer method is restricted to the case of smooth functions. For rapidly oscillating or shock-like functions with large local gradients the truncated Gegenbauer series does not converge unless the number of terms is very large (in fact, prohibitively large in view of the restricted capacity of modern computers). However, the FG method is very accurate when applied on a small sub-interval where the function is smooth. Therefore this algorithm can be efficient in combination with other Fourier methods. In particular, the FG algorithm appears to be very useful in the context of domain decomposition approach being combined with the Local Fourier Basis method (this method is developed for the solution of PDE's in multidomain regions in [5, 6, 7]). These results will be reported elsewhere.

References

[1] D. Gottlieb, Chi-Wang Shu, A. Solomonoff, H. Vandeven, On the Gibbs phenomenon I: Recovering exponential accuracy from the Fourier partial sum of a non-periodic analytic function, *ICASE* Report No. 92-4, (1992)

[2] D. Gottlieb, Chi-Wang Shu, Resolution properties of the Fourier method for discontinuous waves, *ICASE* Report No. 92-27, (1992)

[3] D. Gottlieb, Chi-Wang Shu, On the Gibbs phenomenon III: recovering exponential accuracy in a sub-interval from a spectral sum of a piecewice analytic function. *SIAM J. Numer. Anal.*, to appear.

[4] L. Vozovoi, A.Weill, Spectrally accurate solution of non-periodic differential equations by the Fourier-Gegenbauer method, to appear.

[5] Israeli M., Vozovoi L., Averbuch A., Domain Decomposition Methods for Solving Parabolic PDEs on Multiprocessors, *Appl. Numer. Mathem.*, Vol.12, N. 1-3, (1993), pp.193-212

[6] Israeli M., Vozovoi L., Averbuch A., Spectral Multidomain technique with Local Fourier Basis, *Journal of Scientific Computing*, Vol. 8, No. 2, pp. 135-149, June 1993.

[7] M. Israeli, L. Vozovoi, A. Averbuch, Parallelizing Implicit Algorithms for Evolution Equations by Parabolic Domain Decomposition, *Journal of Scientific Computing*, Vol. 8, No. 2, pp. 151-166, June 1993.

[8] G. Skölermo, A Fourier method for numerical solution of Poisson's equation, *Math. Comput.* (USA), **29**, No 131, (1975), pp. 697-711.

[9] M. Abramowitz, I.A. Stegun, Handbook of Mathematical Functions, Dover, 1970.

[10] H. Bateman, *Higher Transcendental Functions*, Vol.2, McGraw-Hill, 1953.

[11] D. Gottlieb, S.A. Orszag, Numerical analysis of spectral methods:theory and applications, CBMS-NSF Regional Conference Series in Applied Mathematics, *SIAM*, (1977).

[12] P.J. Roache, A Pseudo-Spectral FFT Technique for non-periodic problems, *J. Gomp. Phys.*, **27**, (1978), p.204-220.

[13] L.V. Kantorovich, V.I. Krylov, Approximated methods of higher analysis, Groningen, the Netherlands, 1958.